Vienna Congress on Recent Advances in
Earthquake Engineering and Structural Dynamics 2013 (VEESD 2013)
C. Adam, R. Heuer, W. Lenhardt & C. Schranz (eds)
28-30 August 2013, Vienna, Austria
Paper No. 284

Seismic mitigation performance of multiple nonlinear energy sinks attached to a large-scale nine-story test structure

J. Luo[1], N.E. Wierschem[1], S.A. Hubbard[2], L.A. Fahnestock[1], D.D. Quinn[3], D.M. McFarland[2], B.F. Spencer Jr. [1], A.F. Vakakis[4] and L.A. Bergman[2]

[1] Department of Civil and Environmental Engineering, University of Illinois at Urbana-Champaign, Illinois, USA
[2] Department of Aerospace Engineering, University of Illinois at Urbana-Champaign, Illinois, USA
[3] Department of Mechanical Engineering, The University of Akron, Ohio, USA
[4] Department of Mechanical Science and Engineering, University of Illinois at Urbana-Champaign, Illinois, USA

Abstract. This paper reports an experimental study of innovative passive vibration mitigation devices, nonlinear energy sinks (NESs), installed on a large-scale nine-story test structure. Two different types of the devices were designed and tested. One type employs a nearly cubic restoring force provided by novel nonlinear rubber springs, while the other type features a relative small but nearly linear restoring force in conjunction with single-sided, strongly nonlinear vibro-impacts. Shake table tests using various scaling levels of three historic ground motions were performed. Comparison of multiple structural demands from the tests with the NESs in activated and inactivated configurations demonstrates that these devices can effectively and robustly alleviate multiple structural demands under different scaling levels of ground motions by means of dissipating and redistributing the earthquake-induced vibration energy.

Keywords: Passive control; Nonlinear Stiffness; Shake table test; Seismic mitigation; Energy dissipation

1 INTRODUCTION

Passive vibration control devices have been extensively investigated as an important category of structural control strategies during the past several decades. These devices protect infrastructure by means of alleviating the structural vibration response from extreme loads of earthquakes, blasts and winds. Many of them are supplementary damping devices that can enhance the capacity of structures to dissipate vibration energy. This is typically achieved by either directly convert the kinetic energy to heat through various metallic, frictional and viscoelastic dampers, or direct the energy to dynamic devices such as tuned-mass damper (TMD) and tuned-liquid damper (TLD) (Housner et al. 1997).

In recent years, a novel passive vibration mitigation device, nonlinear energy sink (NES), has been extensively investigated by the authors through analytical, numerical and experimental studies. Distinguished from traditional linear vibration absorbers like the TMDs, these devices employ essentially nonlinear stiffness components that are introduced intentionally in the design stage. When attached to a primary structure, these devices can passively absorb and locally dissipate the vibration energy of the structure in a highly efficient and rapid fashion through passive Targeted Energy Transfer (TET) strategies (Gendelman et al. 2001, Vakakis and Gendelman 2001). Because of the essentially nonlinear stiffness, the NES has no preferential resonant frequency and thus can resonantly interact with multiple structural modes in a broad frequency band to absorb and dissipate energy. Besides dissipating energy by itself, the NES can also couple structural modes together and mobilize energy redistribution from low frequency modes to high frequency modes, where the intrinsic damping of the primary structure dissipates energy more efficiently. Consequently, these vibration

mitigation devices can significantly enhance the apparent damping performance of the primary structure to which they are attached.

Researchers have investigated NES devices with various design types at different scales through analytical and experimental studies. The original form of the device, denoted as Type I NESs, consists of a single-degree-of-freedom moving mass block coupled to the base structure through a nonlinear stiffness component and a linear viscous damping component. Another type is the Type III NES that is a two-degree-of-freedom device composed of two-nested Type I NESs. The Type I and III NESs were physically designed using transverse wires as the nonlinear stiffness components to provide the essentially nonlinear restoring force. Different from these two types that use smoothly nonlinear restoring force, single-sided vibro-impact NES (SSVI NES) employs non-smooth vibro-impacts on a single-sided stopper fixed on the structure. These types of the NES were experimentally studied on a two-story bench-scale test structure (Quinn et al. 2012, Wierschem et al. 2012, AL-Shudeifat et al. 2013). Based on the success of these small-scale studies, an innovative Type III NES employing specially shaped elastomeric bumpers was designed and tested on a six-story medium-sized test structure (Luo et al. 2012, Wierschem et al. 2012).

On the basis of all these previous investigations, a large-scale nine-story steel frame equipped with four Type I NESs and two SSVI NESs were designed and constructed for the purpose of proving the applicability of the NES technology to civil engineering structures. A series of large-scale experiments were conducted on this structure-device system using various forms of external loading. To investigate the performance of the NESs in seismic mitigation, shake table tests using historic seismic ground motions were conducted and the performance of the NESs in seismic mitigation is reported in this paper.

2 TEST STRUCTURE AND NONLINEAR ENERGY SINKS

2.1 Nine-story test structure

A large-scale model building structure was designed and constructed recently as a test bed to experimentally prove the applicability of the NES technology to civil structures. This structure is a roughly five-meter-high, ten-ton, nine-story steel frame incorporating totally six NESs. Figure 1a shows the structure fixed on the shake table. This frame has one base plate and nine floor plates supported by eight columns at every story. The plates and columns are made of steel and assembled by bolt connections. The planar dimension and thickness of the plates are listed in Table 1. Columns of the frame have a rectangular cross-section with large aspect ratio that leads to substantially different moments of inertia about the two principal axes. The height, width and thickness of the columns are summarized in Table 1. All of the column cross-sections are oriented in the same direction and the long sides of all the cross-sections are placed parallel to the long sides of the floor plan. This feature of the design results in very different lateral stiffness about the strong and weak axes of the structure. In the experiment, the structure is exited along the direction shown in Figure 1a so that it can bend about its weak axis. Due to its much higher lateral stiffness about the strong axis, the minor torsional and strong-axis responses caused by the asymmetries existing in the structure and loading can be neglected and the structure essentially vibrates translationally along the loading direction. In addition, to allow the structure to elastically vibrate with relatively large amplitudes, the columns are made of high-strength steel that has a yield strength around 690 MPa.

Table 1. Dimensions of components of nine-story test structure

Plates (floor)	Planar dimension (m × m)	Thickness (mm)	Columns (story)	Height (m)	Width (m)	Thickness (mm)
Base	2.90 × 1.22	44.4	1st	0.635	0.191	14.3
1st to 7th	2.74 × 1.22	38.1	2nd to 9th	0.483	0.140	14.3
8th to 9th	2.74 × 1.22	44.4				

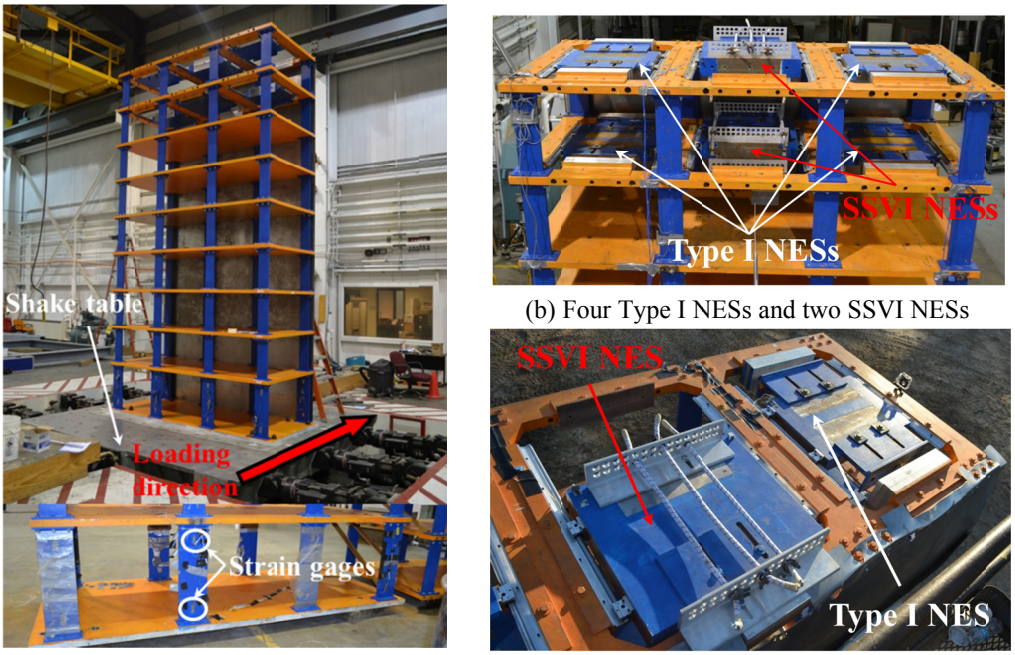

(a) Nine-story test structure on shake table

(b) Four Type I NESs and two SSVI NESs

(c) Close-up view of SSVI and Type I NESs

Figure 1. Nine-story test structure equipped with four Type I NESs and two SSVI NESs.

As the most important design feature of the structure, each of the eighth and ninth floor plates has three cutouts and one NES device is installed inside each cutout. As shown in Figure 1b, totally six NESs are installed in the top two floors. In addition, the mass of the NESs is basically equal to the mass of the removed plates from the cutouts. Thus in this design, part of the structural mass is used as the movable mass of the NESs in a smart way without superimposing additional mass to the structure. Moreover, because the NESs are installed inside the floor plates, they take little story space between the two adjacent floor plates. These design features in terms of the usage of mass and space realize a "non-parasitic" design concept emphasizing that the incorporation of the devices should not affect the normal state and functionality of the building structure.

2.2 Type I and single-sided vibro-impact nonlinear energy sinks

The multiple NESs equipped to the structure include four Type I NESs in the four side cutouts and two single-sided vibro-impact NES (SSVI NESs) in the two central cutouts, as shown in Figure 1b and c. A phenomenological model of the system is shown in Figure 2.

Conceptually, the Type I NES consists of a single-degree-of-freedom moving mass block in the presence of linear viscous damping and essentially nonlinear stiffness components (McFarland et al. 2005, Quinn et al. 2012). The moving mass block is realized by a 406×572×70 mm^3 steel block

equipped with two bushing bearings on each side. One matching rail of the bearings is mounted on each side of the floor plate inside the cutout space. In the operating condition, the mass block moves back and forth along the loading direction, facilitated by the bearings and rails. The nonlinear stiffness components were previously realized by transverse wires without no pretension or slack. In this large-scale design, pyramid-shaped compressive rubber springs are used to provide the nearly cubic stiffness to the NES mass. The rubber springs are installed on both sides of the mass block, along its direction of motion. At rest the tips of the pyramid-shaped springs are exactly in contact with the steel block, but are not pre-compressed. Under excitation, the steel block slides on the rails and alternately compresses the spring on either side as the direction of motion changes. The deformed spring will apply a nonlinear restoring force to the mass block compressing it. When the spring on one side is compressed, a gap opens on the other side between the mass and the spring. The frictional damping between the bearings and rails is used as the main damping source of the device. Note that all the four Type I NESs have the same mass and the two on the same floor have the same design value of stiffness.

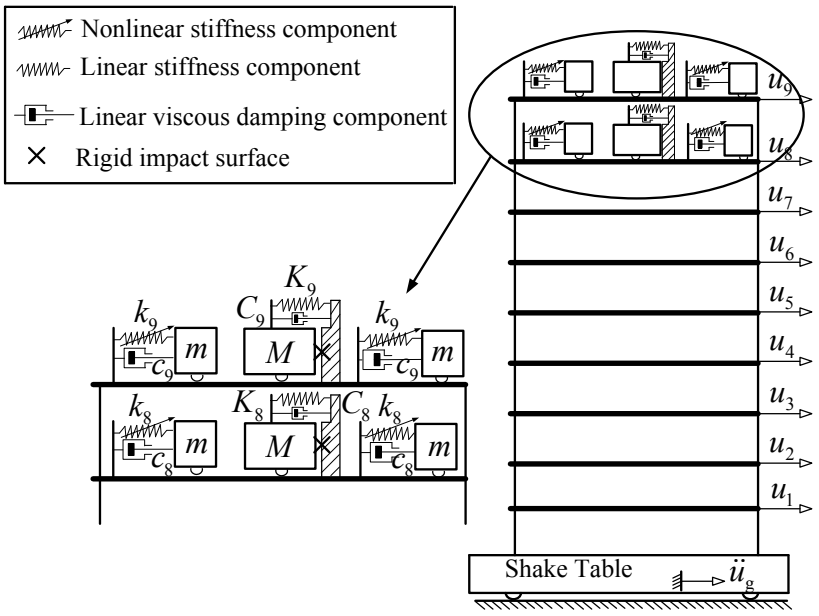

Figure 2. Phenomenological model of the structure-device system.

The SSVI NES is composed of a moving mass block connected to the structure through a linear stiffness component and a linear viscous damping component. As its most important feature, a rigid stopper is placed on one side of the moving mass. In its operating condition, the moving mass impacts the stopper, leading to significant scattering and dissipation of the vibration energy of the structure (AL-Shudeifat et al. 2012). The moving mass block of the SSVI NES is a 546×635×114 mm^3 steel block that has a mass of 340 kg sliding on two rails. Aluminium angles drilled with round holes are fixed to the moving mass block and the floor plate containing the NESs. As the physical realization of the linear stiffness component, elastic cords are used to link the mass block to the floor plate. These cords are fed through the holes on the aluminium angles with saddle clamps on the two ends.

The design values of the stiffness components of the two types of NESs are determined through numerical optimization for the purpose of maximizing the apparent damping of the fundamental structural mode under an impulsive loading. The specific design values of the mass and stiffness of the NES devices are summarized in Table 2.

Table 2. Design values of parameters of NESs

	Mass (kg)	Mass ratio (% of the system)	Stiffness coefficient
Type I NESs on 8th floor	150 for each	1.5 for each	7.56×10^8 N/m^3 for each
Type I NESs on 9th floor	150 for each	1.5 for each	1.07×10^8 N/m^3 for each
SSVI NES on 8th floor	340	3.4	14546 N/m
SSVI NES on 9th floor	340	3.4	12219 N/m

3 SHAKE TABLE TESTING USING HISTORIC GROUND MOTION RECORDS

3.1 Experimental setup

To experimentally investigate the performance of the NES devices in seismic mitigation, large-scale shake table tests using historic ground motion records were conducted at the U.S. Army Engineer Research and Development Center (ERDC), Construction Engineering Research Laboratory (CERL) in Champaign, Illinois. PCB® accelerometers are attached to the base and floor plates of the structure and also the NESs to collect acceleration signals. Uniaxial strain gages were vertically placed on the first-story columns to measure the normal strain of the exterior fibers near the column top and bottom, as shown in Figure 1a.

3.2 Historic seismic ground motions

Table 3 lists the important parameters of the three historic ground motion records used in the shake table testing. To protect the test structure from inelastic deformation, each of the original ground motion was linearly scaled down into five levels with lower amplitudes. The first and second earthquakes are typical near-fault pulse-type earthquakes. The structure-device system was tested using the three ground motion records at each scaling level. Tests on the structure with the NESs in both locked and unlocked configurations were performed, to aid the direction comparison of the structural responses.

Table 3. Historic seismic ground motions used in shake table testing

Record No.	Historic Earthquake	Magnitude	Component \station	Original PGA (g)	Scaling levels (%)	Distance to Fault (km)	Soil Type (USGS)
EQ1	1995 Kobe	6.9	KJM000 0 KJMA	0.821	3.05, 6.09, 11.33, 16.44, 21.44	0.6	B
EQ2	1994 Northridge	6.7	RRS228 77 Rinaldi	0.838	5.97, 10.74, 21.00, 35.20, 43.44	7.1	C
EQ3	1940 Imperial Valley	7.0	I-ELC180 117	0.313	8.31, 15.97, 34.82, 51.12, 60.70	8.3	C

3.3 Experimental results and analysis

Figure 3 to Figure 5 present the experimental results of multiple structural responses under the three seismic ground motions. In each figure, subfigure (a) shows the time history of the unscaled original ground motion record. Subfigures (b) to (d) illustrate time histories of three types of structural response from the tests with the NESs in both locked and unlocked configurations. In subfigure (e), the ratios between the controlled and uncontrolled structural responses are presented at all scaling

levels. The presented structural responses include root-mean-square (RMS) and peak values of first-story column strain, base shear force, base overturning moment and top-floor drift. The base shear force and base overturning moment are calculated using the measured acceleration. The top-floor drift is calculated using the measured acceleration by a procedure employing time integration in conjunction with low and high-pass filtering to eliminate the baseline drift and noise (Boore and Bommer, 2004). The first-story column strain is measured from the strain gage attached to the column.

The time histories of the first and second earthquakes (EQ1 and EQ2 in Table 3) exhibit typical near-fault pulse-type ground motions that have a short duration and high peaks of acceleration at the beginning followed by fast decayed amplitudes. Thus they excite the structure with high input energy at the beginning in a nearly impulsive manner. On the contrary, the ground motion of the third earthquake has a long duration and several times of energy release, so it excites the structure with a more uniformly distributed energy during its period.

As seen from subfigure (e) of Figure 3 and Figure 4, for the first and second ground motions, the RMS values of multiple structural responses are reduced by more than 50% due to the effect of the NES devices. As shown in the time histories of the structural responses, the duration of the residual responses after the short period of the ground motion is significantly shortened because of the enhanced energy dissipation introduced by the NESs. For example, the ground motion of the first earthquake decays to almost zero in around 20 second and the remained structural responses diminish to almost zero right after the end of the ground motion. However, when the NESs are inactivated, the amplitudes of the residual responses are still significant at the end of the 40-second window. In addition, an inspection on the frequency of the responses reveals that when the NESs are activated, the low-amplitude responses exhibit a high vibration frequency. This phenomenon indicates the ability of the NESs to redistribute vibration energy from low-frequency modes to high-frequency modes. This facilitates the alleviation of responses because for this test structure under base motion, the modal contribution factor of the fundamental mode is calculated to be more than 95% (Chopra 2006). Therefore, when the vibration energy is shifted from the fundamental mode to higher modes, its contribution to the structural responses becomes much smaller. Moreover, the intrinsic damping of the structure dissipates vibration energy more rapidly at the higher modes.

The reduction of the peak values of the structural responses is less effective than that of the time-averaged values, especially for the two pulse-type earthquakes. The reason is that for the NES devices, the motion of the mass is required for the response reduction. However, as demonstrated by the time histories, the structural responses under the high-amplitude pulses reach the peaks in a very short time that is smaller than the characteristic time scale of the NES response. Therefore, the reduction of the structural responses during the short duration of the pulse-type ground motion is not as much as that of the residual responses after the ground motion. As Figure 5 (a) shows, different from the first and second earthquakes, the third earthquake has a long duration with slowly released energy. Under this excitation, the NESs have sufficient time to respond and become active. As shown by the time histories of the structural responses, during several times of major energy release, the alleviation of the peak responses is more effective than that of the first two earthquakes. The residual responses right after the duration of the ground motion is reduced to almost zero, which is similar to the performance under the first two earthquakes. In subfigure (e) of Figure 3 to Figure 5, for all the three earthquakes, the performance of the NES devices in response reduction is demonstrated by tests using ground motions with different scaling levels. Most structural responses exhibit a consistent reduction over the scaling range without large variation. This performance demonstrates that the NES devices can accommodate to ground motions with various intensities and reduce the strutrual response in a highly effective and robust fashion. This is a highly desired property considering the uncertainties of the ground motion.

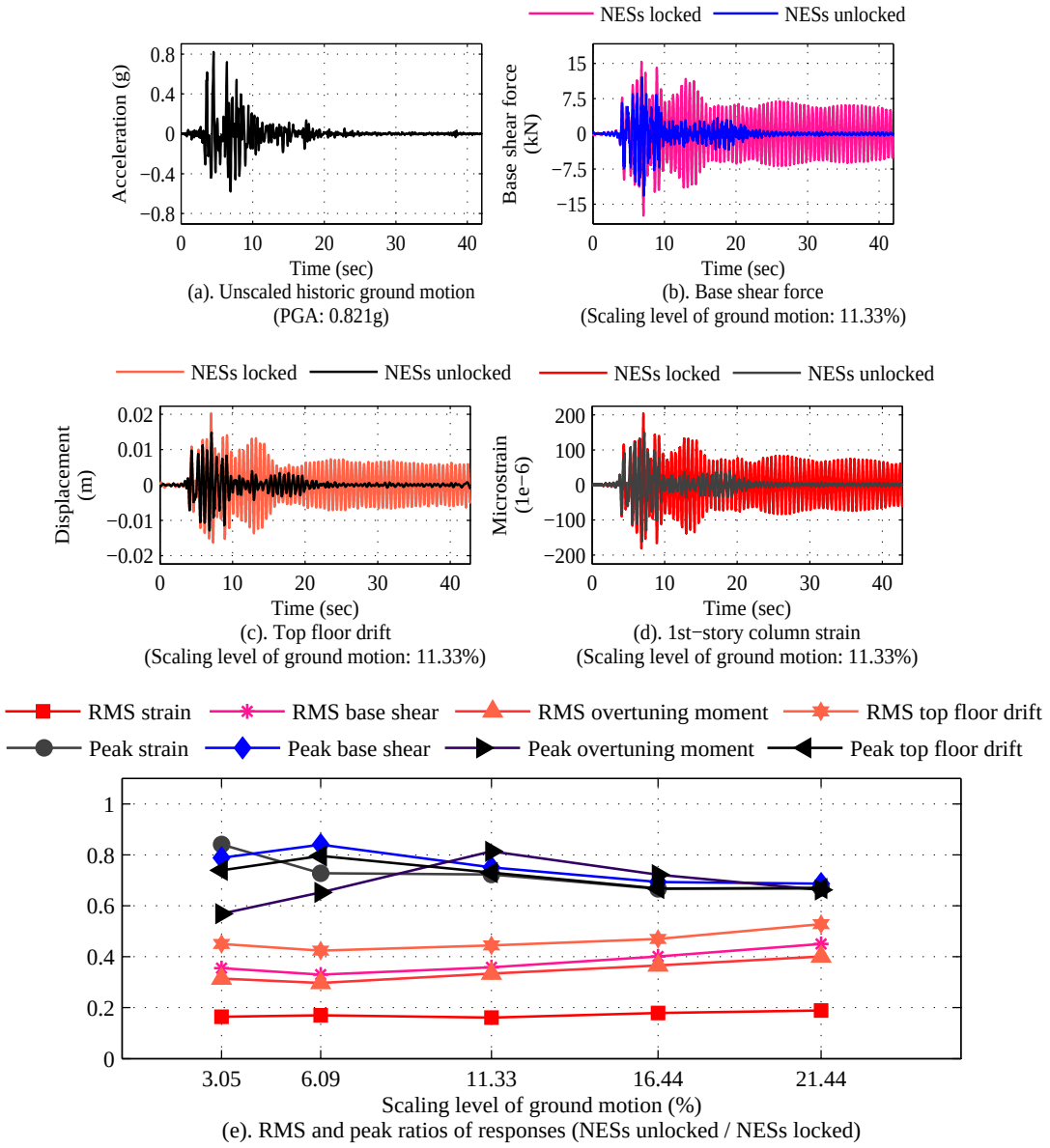

Figure 3. Experimental results of seismic testing using EQ1.

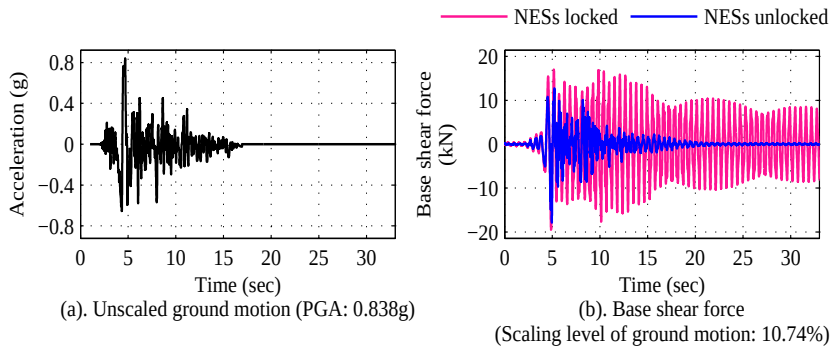

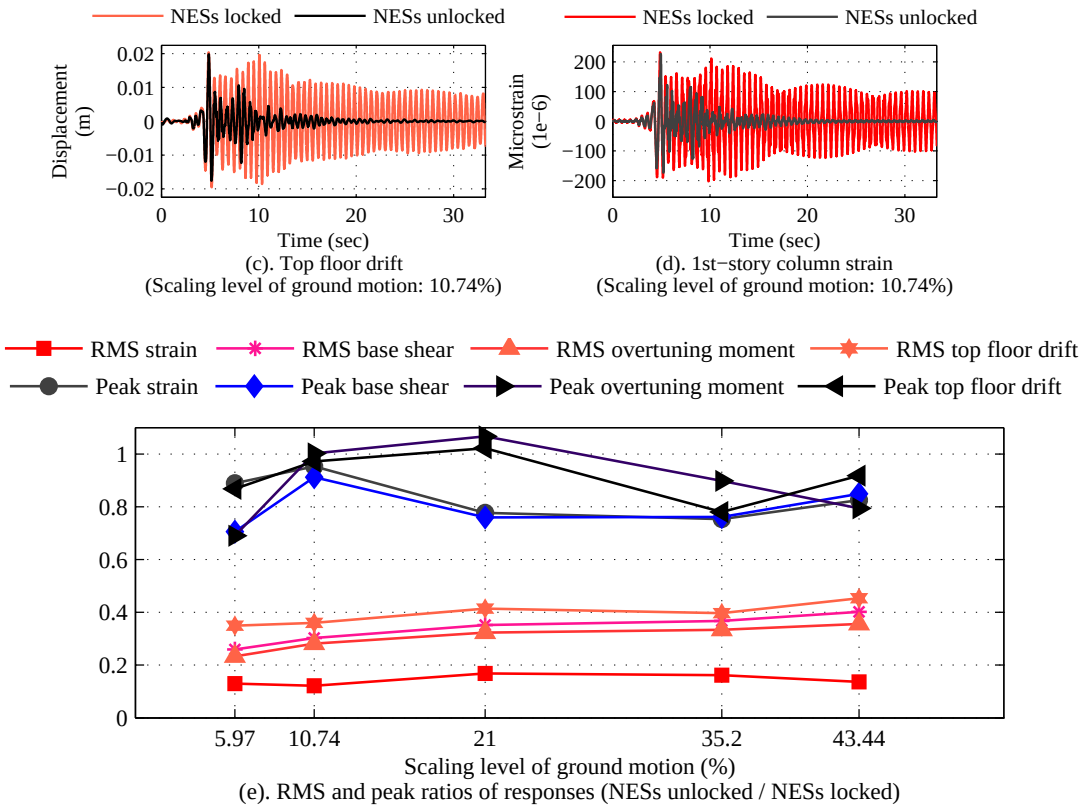

Figure 4. Experimental results of seismic testing using EQ2.

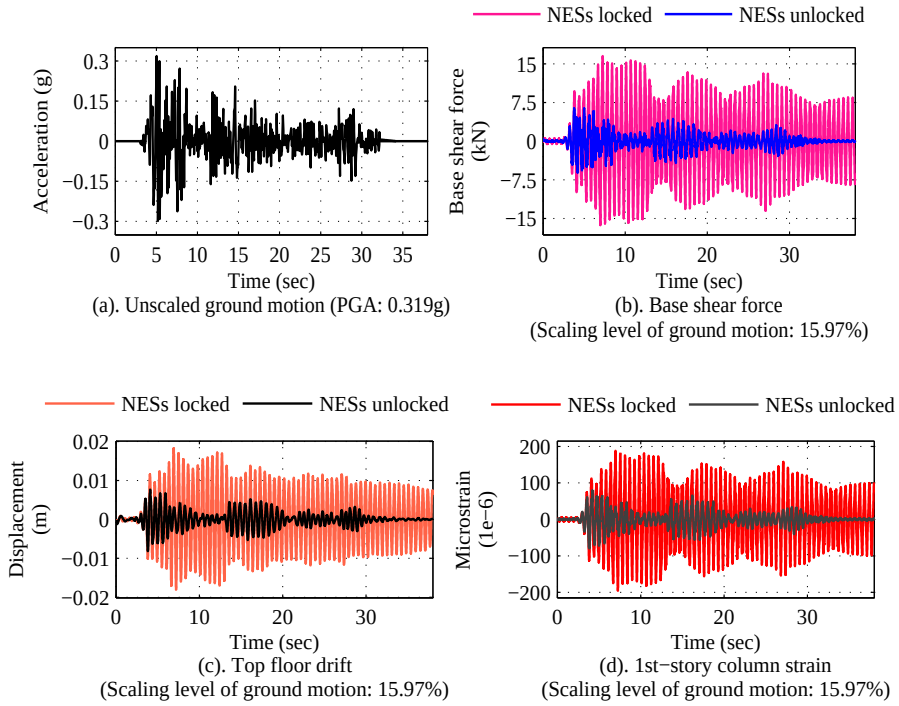

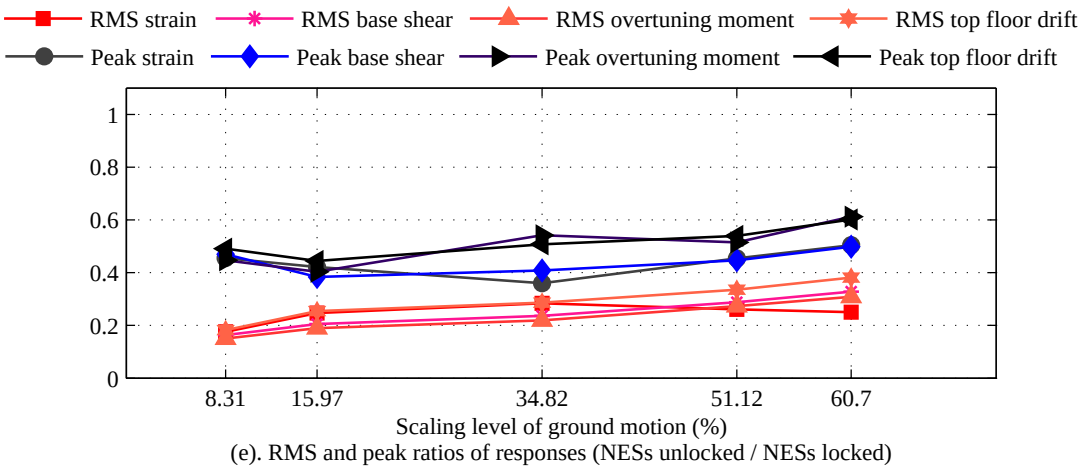

(e). RMS and peak ratios of responses (NESs unlocked / NESs locked)

Figure 5. Experimental results of seismic testing using EQ3.

4 CONCLUSIONS

This paper reports an experimental study of the seismic mitigation performance of nonlinear energy sinks (NESs) as innovative passive vibration mitigation devices. Four Type I NESs and two single-sided vibro-impact NESs are installed on a large-scale nine-story test structure. Shake table tests using various scaling levels of three historic ground motions were performed with the devices in both activated and inactivated states. Experimental results demonstrate that the multiple structural demands including base shear force, base overturning moment, top-floor drift and first-story column strain can be significantly reduced due to the effect of the NESs in dissipating and redistributing vibration energy. The performance of the devices in seismic mitigation is shown to be robust by the consistent alleviation of the structural responses at multiple scaling levels. While the averaged structural responses are substantially reduced for all the three earthquakes, the performance in reducing the peak responses is affected by the type of the ground motion.

5 ACKNOWLEDGEMENTS

This research program is sponsored by the Defense Advanced Research Projects Agency through grant HR0011–10–1–0077; Dr. Aaron Lazarus is the program manager. The content of this paper does not necessarily reflect the position or the policy of the Government, and no official endorsement should be inferred.

REFERENCES

Al-Shudeifat, M.A., Wierschem, N.E., Quinn, D.D., Vakakis, A.F., Bergman, L.A., and Spencer Jr., B.F. (2012). Numerical and experimental investigation of a highly effective single-sided vibro-impact nonlinear energy sink for shock mitigation. *International Journal of Non-Linear Dynamics* **52**(0):96-109.

Boore D.M. and Bommer J.J. (2005). Processing of strong-motion accelerograms: needs, options and consequences. *Soil Dynamics and Earthquake Engineering* **25**(2):93-115.

Chopra A.K. (2006). Dynamics of Structures: Theory and Applications to Earthquake Engineering. Third edition. Prentice Hall.

Gendelman, O., Manevitch, L.I., Vakakis, A.F., and Closkey, R.M. (2001). Energy pumping in nonlinear mechanical oscillators: Part I—Dynamics of the underlying Hamiltonian systems. *Journal of Applied Mechanics* **68**(1): 34-41.

Housner G.W., Bergman L.A., Caughey T.K., Chassiakos A.G., Claus R.O., Masri S.F., Skelton R.E., Soong T.T., Spencer B.F., and Yao. J.T.P. (1997). Structural control: Past, present, and future. *Journal of Engineering Mechanics (ASCE)* **123**(9):897–971.

Luo J., Wierschem, N.E., Fahnestock L.A., Bergman L.A., Spencer Jr, B.F., Al-Shudeifat M.A., McFarland, D.M., Quinn D.D., and Vakakis A.F. (2012). Realization of a strongly nonlinear vibration mitigation device using elastomeric bumpers. *Journal of Engineering Mechanics (ASCE)*. (*In review*).

McFarland D.M., Bergman L.A., and Vakakis A.F. (2005). Experimental study of non-linear energy pumping occurring at a single fast frequency. *International Journal of Non-Linear Mechanics* **40**(6):891-899.

Quinn, D.D., Hubbard, S.A., Wierschem N.E., AL-Shudeifat, M.A., Ott, R.J., Luo, J., Spencer Jr., B.F., McFarland, D.F., Vakakis, A.F., and Bergman, L.A. (2012). Equivalent modal damping, stiffening and energy exchanges in multi-degree-of-freedom systems with strongly nonlinear attachments. *Proceedings of the Institution of Mechanical Engineers, Part K: Journal of Multi-body Dynamics* **226**(2): 122-146.

Vakakis, A.F. and Gendelman, O. (2001). Energy pumping in nonlinear mechanical oscillators: Part II—Resonance Capture. *Journal of Applied Mechanics* **68**(1): 34-41.

Wierschem, N.E., Quinn, D.D., Hubbard, S.A., Al-Shudeifat, M.A., McFarland, D. M., Luo, J., Fahnestock L.A., Vakakis, A.F., Bergman, L.A., and Spencer Jr., B.F. (2011). Passive damping enhancement of a two-degree-of-freedom system through a strongly nonlinear two-degree-of-freedom attachment. *Journal of Sound and Vibration*. **331**(25): 5393-5407.

Wierschem, N.E., Luo, J., Al-Shudeifat, M.A., Hubbard, S.A., Ott, R.J., Fahnestock L.A., Quinn, D.D., McFarland, D.M., Spencer Jr., B.F., Vakakis, A.F., and Bergman, L.A. (2012). Experimental resting and numerical simulation of a six-story structure incorporating a two-degree-of-freedom nonlinear energy sink. *Journal of Structural Engineering (ASCE)*. (*In review*).